JOURNAL OF THERMOPHYSICS AND HEAT TRANSFER
Vol. 22, No. 3, July–September 2008

Modeling Laser-Induced Plasma Expansion Under Equilibrium Conditions

A. R. Casavola*
University of Bologna, 40136 Bologna, Italy
G. Colonna†
Institute of Inorganic Methodologies and Plasmas CNR, 70126 Bari, Italy
A. Cristofolini‡ and C. A. Borghi§
University of Bologna, 40136 Bologna, Italy
and
M. Capitelli¶
University of Bari, 70126 Bari, Italy

DOI: 10.2514/1.33507

A theoretical investigation of the expansion of the plasma, produced by a nanosecond laser pulse hitting a titanium metallic target, has been carried out. The study is oriented to understand the interaction of the plasma plume with the surrounding gas (air) not only from the fluid dynamic point of view, but also considering the effects of chemical reactions. To this purpose, a 2-D solver of the Euler equations has been developed and self-consistently coupled with the local thermodynamic equilibrium calculation. The results show the plasma confinement due to the ambient gas and the appearance of metallic oxides in proximity of the plume border.

Nomenclature

H_f	=	chemical energy
L	=	target dimension
$\bar{M}$	=	mean molecular mass
nsp	=	total number of species
P	=	pressure
R	=	gas constant
T	=	temperature
t	=	time
U	=	internal energy
u	=	flow speed in the x direction
v	=	flow speed in the y direction
z_{d_x}	=	source term for density
$z_{d_{xi}}$	=	density produced for each species in the time unit
z_{e_x}	=	source term for energy
z_{v_x}	=	source term for velocity u
ε	=	total energy per unit mass
ρ	=	mass density
ρ_i	=	mass density of the species i

Presented as Paper 4593 at the 38th AIAA Plasmadynamics and Lasers Conference in conjunction with the 16th International Conference on MHD Energy Conversion, Miami, Florida, 25–28 June 2007; received 17 July 2007; revision received 10 December 2007; accepted for publication 16 December 2007.

*Fellowship Researcher, Dipartimento di Ingegneria Elettrica Viale Risorgimento, 2; annarita.casavola@ba.imip.cnr.it, Member AIAA.

†Researcher, Consiglio Nazionale delle Ricerche, Istituto di Metodologie Inorganiche e Plasmi. AIAA Member.

‡Associate Professor, Dipartimento di Ingegneria Elettrica Viale Risorgimento. Member AIAA.

§Full Professor, Dipartimento di Ingegneria Elettrica Viale Risorgimento. Member AIAA.

¶Full Professor, Department of Chemistry. Fellow AIAA.

I. Introduction

LASER-INDUCED plasma (LIP) is a topic of growing interest in different fields such as material processing, diagnostic techniques, and space applications. Pulsed laser deposition (PLD) has been successfully employed for the deposition of thin films of classical and novel materials [1,2]. The possibility of producing species in LIP with electronic states far from chemical equilibrium enlarges the potential of making novel materials that would be unattainable under thermal conditions. LIP technological applications require a parallel investigation of the plasma plume from a fundamental point of view. Indeed, while the generation of LIP requires a simple experimental setup, the LIP theoretical investigation requires strong efforts in fluid dynamics and chemical kinetic models.

Many numerical approaches (see, for example, [3–6]) have been developed to adequately describe the plasma expansion, and a strong linking with experimental research [7,8] has improved the knowledge of this complex phenomenon. The main difficulty in modeling LIP expansion is that the plume dynamics and plasma chemical reactions should be investigated and ultimately modeled together, in a coupled fashion, considering not only the evaporated species, but also the interactions with the environment.

In this context, a 2-D fluid-dynamic approach, taking into account the role of chemical processes, is proposed. Euler equations are used to simulate the plasma in the early stage of its evolution, including a detailed chemical scheme. While in high vacuum reactors the plume expands essentially perpendicularly to the target with a very small angular dispersion, and therefore one-dimensional models adequately describe the plume dynamics [9–11], in high pressure environments (such as air or water) the 1-D approach strongly overextimates the flow speed, because the real expansion is practically spherical. In this case a 2-D model is essential to describe the plume confinement due to the ambient gas.

LIP setup is used also as an elemental analysis [12] and on-line control of laser-matter interaction [8], in the so-called laser-induced breakdown spectroscopy (LIBS) technique. The flexibility of LIBS allows its use in a wide range of applications as environmental heavy metal contaminations [13], monitoring of industrial processes [14], space exploration [15], artwork analysis [16], defense application [17], and so on. The possibility of employing LIBS in a double-pulse mode leads to the extension of this kind of in situ diagnostic in a water

submerged environment [18], where conventional analytical techniques are unfeasible. Despite the importance of underwater LIBS applications, few results have been obtained in such an environment [18–24].

When a nanosecond laser pulse is focused on a submerged target, a consistent amount of the laser energy is spent in mechanical effects, resulting principally in the formation of a cavitation bubble [25]. Even if there is enough laser energy to form the plasma, due to the interaction of the ablated particle with water, the plasma is rapidly cooled by electron-ion radiative recombination and by chemical reactions so that the single-pulse LIP spectral emission signal is very short and noisy [26]. When a second pulse strikes the target surface before the bubble produced by the first pulse collapses, the LIBS signal is enhanced and shows behaviors similar to single-pulse LIBS in air. It has been observed both theoretically [27] and experimentally [18,25,26] that the bubble size strongly affects the emission spectra produced by the second laser pulse, underlying the fact that the bubble dynamics is very relevant for the double-pulse LIBS [28].

A set of experiments [18] by double-pulse LIBS on a submerged target has been performed also to test the feasibility of this kind of application in seawater. On the other hand, a great effort has been given to build a theoretical model able to simulate the experimental observations during the ablation of a metallic titanium target at low pressure [3,7,29,30]. In that system the 1-D fluid dynamics has been coupled with the ionization–recombination kinetics of titanium atoms to obtain a quantitative agreement with optical emission measurements of the plasma temporal evolution. The same approach has been improved to simulate the double-pulse LIBS on metallic titanium in water taking into account the chemical reactions of the ablated material with water vapor environment. To obtain the background conditions inside the vapor bubble, before plasma expansion, and to validate the model with some experimental data, a theoretical study on the bubble dynamics has been done, considering an homogeneous bubble in thermal and chemical equilibrium [27]. All these investigations have used the 1-D plasma expansion model.

In this paper we have developed a 2-D fluid-dynamic model of the plasma expansion coupled with a complete thermochemical equilibrium model for Ti + air and Ti + water systems. We consider the second laser pulse striking the target inside the vapor bubble, which is supposed to be a static system. The bubble lifetime (expansion collapse) has a duration at least in the order of hundreds of microseconds, depending on the laser pulse characteristics (wavelength, energy density, and pulse duration [31]), while the second pulse LIP in water extinguishes in a few microseconds ($<5\ \mu$s). Therefore, it is reasonable to consider the bubble as a stationary environment in which the LIP expands. Because of the high pressure of the ambient gas, local thermodynamic equilibrium can be supposed. This assumption has been confirmed by experimental measurements [32]. Particular attention will be devoted to the effects of a 2-D expansion, the role of plasma processes, and to the role of the chemical interaction between the plume and the ambient gas.

II. Theoretical Model

Because of experimental resolution and sensitivity the description of the plasma dynamics by optical measurements is not exhaustive. The support of theoretical investigation of the plume expansion can give a more complete characterization of the plasma. In this paper we have extended the 1-D model [29,30] in local thermodynamic equilibrium (LTE) approximation to 2-D geometry, solving Euler equations. This approach describes the local thermodynamic model with two state variables (as an example, pressure and temperature, or density and energy). For accurate calculations, we consider a detailed description of the internal degrees of freedom of atoms and molecules. For atoms many electronically excited states have been considered, limited by a cutoff to prevent partition function divergence. For molecules, all available electronically excited states have been included in the calculations considering for each of them the complete rovibrational ladder.

We solve the equations:

$$\frac{\partial \rho}{\partial t} + \frac{\partial \rho u}{\partial x} + \frac{\partial \rho v}{\partial y} = z_{d_x} \tag{1}$$

$$\frac{\partial \rho u}{\partial t} + \frac{\partial u \rho u}{\partial x} + \frac{\partial v \rho u}{\partial y} + \frac{\partial P}{\partial x} = z_{v_x} \tag{2}$$

$$\frac{\partial \rho v}{\partial t} + \frac{\partial v \rho v}{\partial y} + \frac{\partial u \rho v}{\partial x} + \frac{\partial P}{\partial y} = 0 \tag{3}$$

$$\frac{\partial \rho \varepsilon}{\partial t} + \frac{\partial u \rho \varepsilon}{\partial x} + \frac{\partial v \rho \varepsilon}{\partial y} + P\left(\frac{\partial u}{\partial x} + \frac{\partial v}{\partial y}\right) = z_{e_x} \tag{4}$$

The source term z_{e_x} for energy includes the laser heat input into the escaping particles.

There are different models of the ablation process based on laser energy conversion. These models are not very accurate because they do not consider the interaction mechanisms [33]. A different approach consists of describing the evaporation process with an analytical function, derived by optimizing theoretical results with experimental data [3,7]. The ablation rate used in this work has been determined for the fluence range 5 J/cm^2.

The expanding plasma is formed by atoms, ions, and electrons. To study the spatial and temporal evolution of the density of each species i, we have modified the mass conservation Eq. (1) in the form:

$$\frac{\partial \rho_i}{\partial t} + \frac{\partial \rho_i u}{\partial x} + \frac{\partial \rho_i v}{\partial x} = z_{d_{xi}} \tag{5}$$

where ρ_i is the mass density of the species i and z_{dxi} is the density produced for each species in the time unit. To connect the total density of the system and the density of the different species, we have used the relation:

$$\rho = \sum_{i=1}^{\text{nsp}} \rho_i \tag{6}$$

where nsp represents the total number of species.

We have applied these equations to the study of a titanium target expanding in air or in water vapor at different pressures, supposing that the species produced from the target are Ti^+ and e^- both with molar fractions 0.5.

The system of Eqs. (1–6) must be coupled with an equation that connects pressure, temperature, and molecular mass. According to the hypothesis of an ideal gas, the correlation between pressure and temperature can be described by the equation:

$$P = \frac{\rho}{\bar{M}} RT \tag{7}$$

where T is the temperature, $\bar{M}$ is the mean molecular mass, and R is the gas constant. The general expression of total energy per unit mass (ε) is

$$\varepsilon = \frac{3}{2}\frac{RT}{\bar{M}} + \frac{U}{\bar{M}} + \frac{H_f}{\bar{M}} \tag{8}$$

where U is the internal energy and H_f is the chemical energy. For an ideal gas without internal structure and chemical reactions, Eq. (7) is simplified as

$$P = \tfrac{2}{3}\rho\varepsilon \tag{9}$$

Two nonideal contributions to Eq. (9) have been neglected: virial and Debye–Hückel corrections [34]. It has been shown [35,36] that the virial correction is very small for $T > 2000$ K up to 1000 atm, but can be relevant for $T < 300$ K and $P \sim 100$ atm [37], conditions not present in our calculations. The Debye–Hükel correction [34] can be more important, not exceeding in any case the 5%. Our calculations

include the Debye–Hükel theory for self-consistently cutting the atomic partition functions and their derivatives.

The numerical solution of the system of Eqs. (1–7) determines the time-dependent profiles of different macroscopic quantities, such as mass density, temperature, and Mach number between the target and the substrate [3,7,29,30]. We have solved the system of equations numerically, applying an "upwind" space discretization [38], solving alternately in the x direction and y directions, following the operator splitting method [39].

To calculate the thermodynamic quantities and the equilibrium constants we use the statistical thermodynamic approach [40], starting from the partition functions. The partition functions are calculated directly from internal levels, obtained from spectroscopic constants for molecules [41] and from energy levels for the atoms.** In the calculation of partition functions, the effects of quasi-bound vibrorotational states, energy-level completion of the monatomic components, and autoionizing states have been also considered [42]. From partition functions it is possible to calculate the single species thermodynamic properties and the equilibrium constants, and, knowing the gas composition, the mixture thermodynamic functions can be easily determined. The equilibrium composition is calculated using the hierarchical approach described in [43,44]. This method consists of solving one equilibrium equation at a time, following the proper order. The choice of the order in which the reactions are solved is a critical point in the algorithm and determines the speed of convergence. This method is very suitable for fluid-dynamic applications for two reasons. First of all, it does not need inversion of large matrices, and moreover it determines the concentration of majority species very fast, as first stage, and then refines the solution calculating secondary species and traces.

Fluid-dynamic and equilibrium modulus have been coupled following this procedure: in a given time step the fluid-dynamic evolution is calculated neglecting the reactions, then the species concentration is updated, in each grid point, under constant volume and energy constraint.

The fluid-dynamic evolution considers a step adaptive method, to limit the truncation error of all the relevant quantities [38]. The step adapting method is based on the evaluation of the integration errors by comparing the numerical solution with the extrapolation value obtained from previous steps.

III. Results

The effect of chemical reactions on the plume expansion can be studied comparing LTE results with those obtained in the "free-flow" approximation, that is, neglecting the chemical reactions. The calculations have been performed considering different spatial grids. The best results have been obtained with $\Delta = 5 \times 10^{-5}$ m. Anyway, by doubling the grid size the results are very close, showing smoother profiles.

The ablated particles are produced at a constant rate from the target surface for a given release time in the ambient gas (water vapor or air). In the case of a water bubble we suppose that the plasma and vapor particles are confined inside the bubble because the particle exchange through the bubble surface is much slower than the bubble dynamics. On the contrary, in air environment an open boundary condition is supposed, being the plume size smaller than the reactor. For the titanium target the following species can be considered: Ti, Ti^+, TiO, TiO_2, H_2O, H_2, H_2^+, O_2, O_2^+, O_2^-, H, H^+, O, O^-, O^+, O^{+2}, O^{+3}, O^{+4}, OH, OH^+, OH^-, N_2, N_2^+, N_2^-, N, N^+, N^{+2}, N^{+3}, N^{+4}, NO, NO^+, and e^-. Two different sets of initial conditions are used for the different background (in air $T_0 = 30,000$ K, $V_0 = 10^4$ m/s, and $Z_d = 5000$ Kg/m^3/s; in water $T_0 = 20,000$ K, $V_0 = 1 \times 10^4$ cm/s, and $Z_d = 5000$ Kg/m^3/s) to reproduce experimental conditions [29]. The laser pulse duration is of the order of tens of ns. Both in air and water environment, the target is evaporated with the following fractions: 50% Ti^+, 50% e^-. The background pressure varied between 10^{-3} and 1 atm. As initial background conditions we consider local thermodynamic equilibrium at the $T = 300$ K.

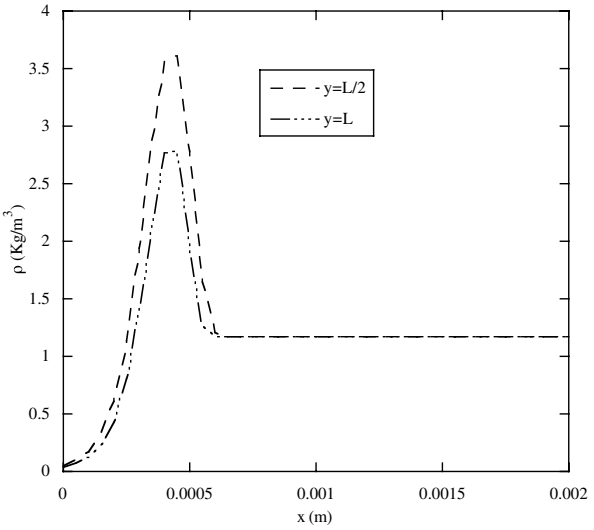

Fig. 1 Mixture density profile as a function of distance from the target after 10^{-7} s from the beginning of the laser pulse at $y = L/2$ and $y = L$. The expansion occurs in air background at 1 atm.

First of all, we will discuss results obtained for the simulation of a titanium plasma expanding in air background. Figure 1 shows the density profile as a function of the distance x from the target at different y position, with L being the dimension of the evaporation region ($L = 0.6$ mm). We report the density profile after 10^{-7} s from the beginning of the laser pulse, with the first one along the normal in the middle of the target ($y = L/2$), and the second one along the normal at the end of the target ($y = L$). Because of the broadening of the plume at the edge of the target during the expansion, a reduction is shown of the mass density as moving apart from the symmetry axes. The effect of the expansion in two dimension can be observed clearly by comparing the density profile obtained with 1-D and 2-D codes, as shown in Fig. 2: for a short time the two models predict the same density, for a longer time peak in the density profile along the symmetry axes is higher in the 1-D model than in the 2-D model.

As a consequence of the equilibrium calculation, during the expansion the titanium ions and the electrons can recombine, depending on the plasma temperature. Figure 3 shows the density

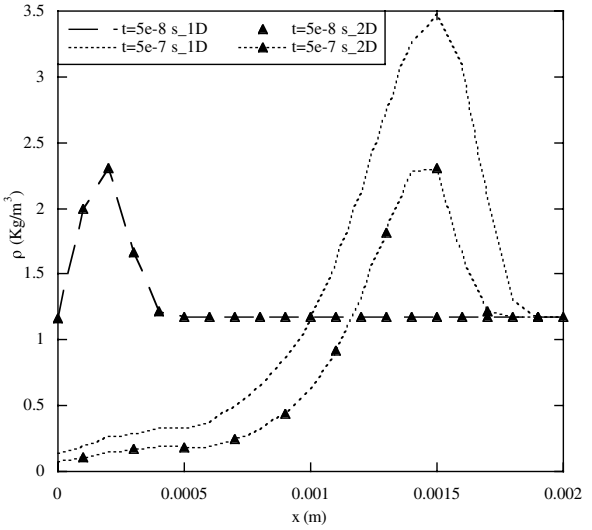

Fig. 2 Mixture density profile as a function of distance from the target after 5×10^{-8} s and 5×10^{-7} s from the beginning of the laser pulse. Comparison between 1-D and 2-D results, obtained along the normal in the middle of the target. The expansion occurs in air background at 1 atm.

**IAEA (International Atomic Energy Agency) database available online at http://www-amdis.iaea.org/ [retrieved 3 March 2008].

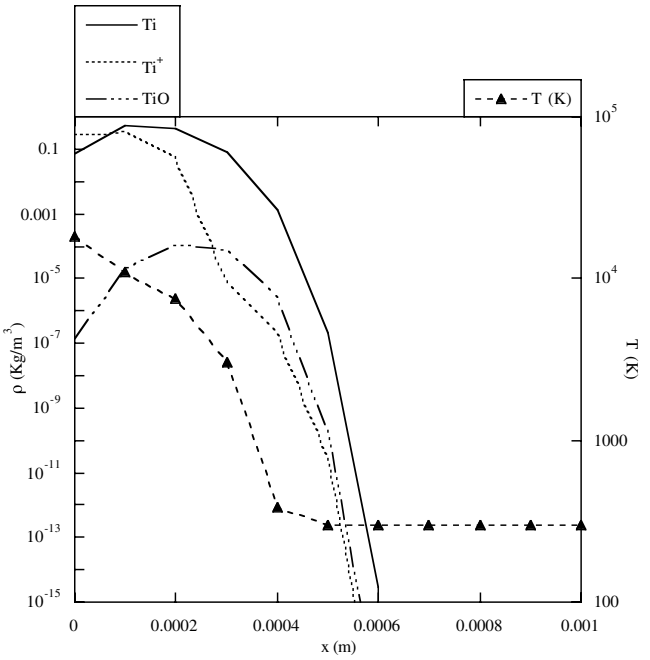

Fig. 3 Density profile of Ti, Ti^+, and TiO as a function of distance from the target after 5×10^{-8} s from the beginning of the laser pulse (on the left), temperature profile as a function of distance from the target after 5×10^{-8} s from the beginning of the laser pulse (on the right) along the normal in the middle of the target. The expansion occurs in air background at 1 atm.

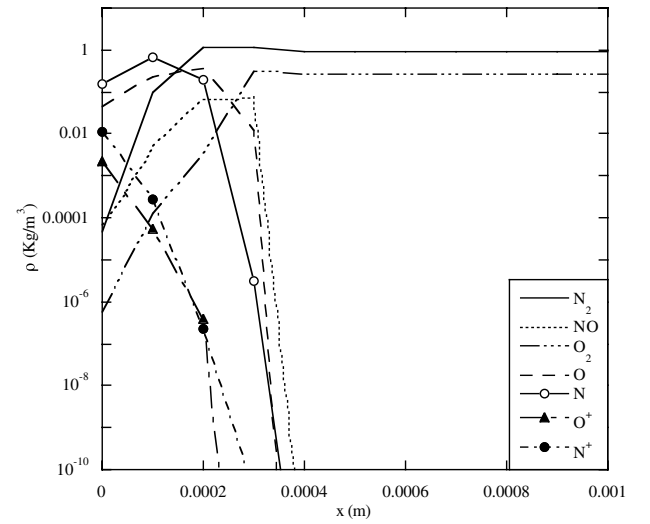

Fig. 4 Density profile of N_2, NO, O_2, O, N, O^+, and N^+ as a function of distance from the target after 5×10^{-8} s from the beginning of the laser pulse along the normal in the middle of the target. The expansion occurs in air background at 1 atm.

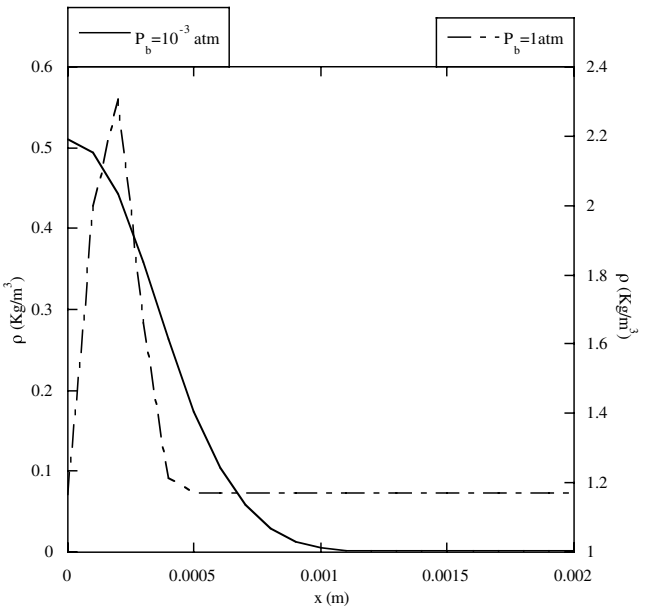

Fig. 5 Mixture density profile as a function of distance from the target after 5×10^{-8} s from the beginning of the laser pulse along the normal in the middle of the target. The expansion occurs in air background at 10^{-3} atm (on the left) and at 1 atm (on the right).

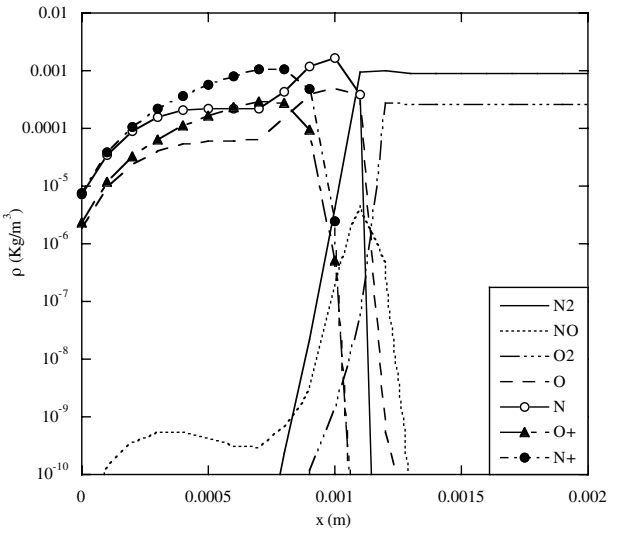

Fig. 6 Density profile of N_2, NO, O_2, O, N, O^+, and N^+ as a function of distance from the target after 5×10^{-8} s from the beginning of the laser pulse along the normal in the middle of the target. The expansion occurs in air background at 10^{-3} atm.

profile of Ti, Ti^+, and TiO after 5×10^{-8} s from the beginning of the laser pulse (on the left), together with the temperature profile (on the right). When temperature decreases the recombination is stronger and atoms and molecules appear.

In Fig. 4 the density profile of some air components is plotted as a function of distance after 5×10^{-8} s from the beginning of the laser pulse. Although the background at 300 K is made of N_2 and O_2, the plasma determines dissociation (N, O), ionization (N^+, O^+) and recombination (NO). In particular, ions are especially present in the hot region of the plume, while NO increases at the front expansion where temperature is lower.

To show the strong effect of gas background pressure on the plume expansion, in Fig. 5 we report a comparison between the density profile after 5×10^{-8} s from the beginning of the laser pulse in the case of background pressures of 1 and 10^{-3} atm. One can observe that the lower background pressure allows a faster expansion and a less confinement effect on the plume. Moreover, the lower background pressure modifies the chemical reactions occurring between the plume and the background, as evident from Fig. 6, leading to a minor recombination effect and to a much higher ion concentration inside the plasma. Therefore the background pressure influences both the fluid-dynamic and the chemical processes occurring during the plasma expansion.

To verify the effect of chemical equilibrium calculation, in Fig. 7 there is a comparison between free flow and "reactive flow" in the case of an expansion against air at 10^{-3} atm. The free flow is a simplified case, supposing infinitely slow chemical rates and therefore no reaction occurs in the time of plume expansion. This plot shows the density as a function of the distance from the target after 5×10^{-7} s from the beginning of the laser pulse. The plume expands in air (N_2 and O_2). Because of the heating of the background as

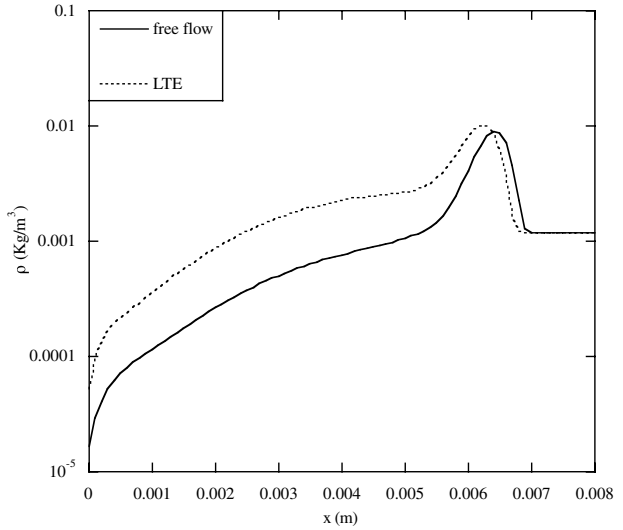

Fig. 7 Mixture density profile as a function of distance from the target after 5×10^{-7} s from the beginning of the laser pulse along the normal in the middle of the target. Comparison between free flow and reactive flow. The expansion occurs in air background at 10^{-3} atm.

plasma expands, chemical reactions can take place. It seems that the introduction of the chemical processes decelerates the flow expansion. This is due to the conversion of translational energy in chemical energy, with a consequent deceleration of the plume front, due to the relevant dissociation of the air molecules. The introduction of chemical processes slows down the translational temperature, so that the plume can move slower than in the case of a frozen system.

Similar results have been obtained by the study of a titanium plasma expanding in a water background. To show the broadening of the plume both in air and in water, in Figs. 8a and 8b the density after 10^{-7} s from the beginning of the laser plot is shown in a 2-D graph (expansion in air in Fig. 8a, expansion in water vapor in Fig. 8b). It is quite interesting to observe the broadening of the plume, which is more evident in the case of water background, and the faster movement of plasma when it expands in air, compared with LIP in water, where there is a strong confinement effect of the plume. Moreover, in both cases a decreasing of the density close to the target can be observed as a consequence of the plume expansion.

As an example in Figs. 9a and 9b the water composition is shown, respectively, in the case of an expansion against 10^{-3} and 1 atm. A strong influence on the species concentration depending on the background pressure is evident, as already shown in the case of expansion in air. In particular, at lower background pressure

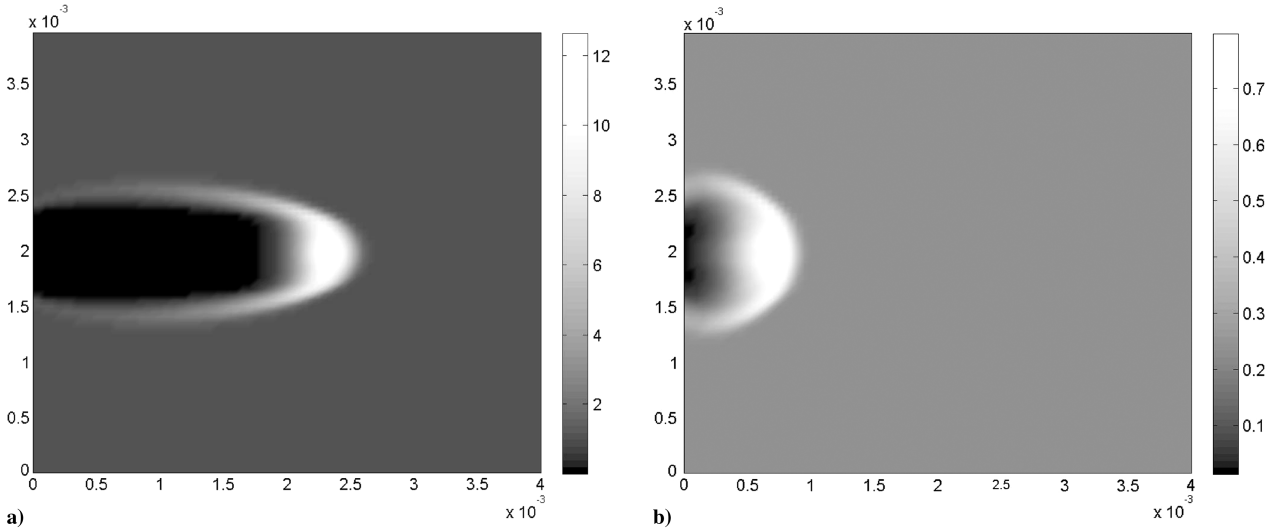

Fig. 8 Two-dimensional mixture density profile (Kg/m^3) after 1×10^{-7} s from the beginning of the laser pulse. Comparison between air background (Fig. 8a) and water vapor background (Fig. 8b). $dx = 5e - 5m$.

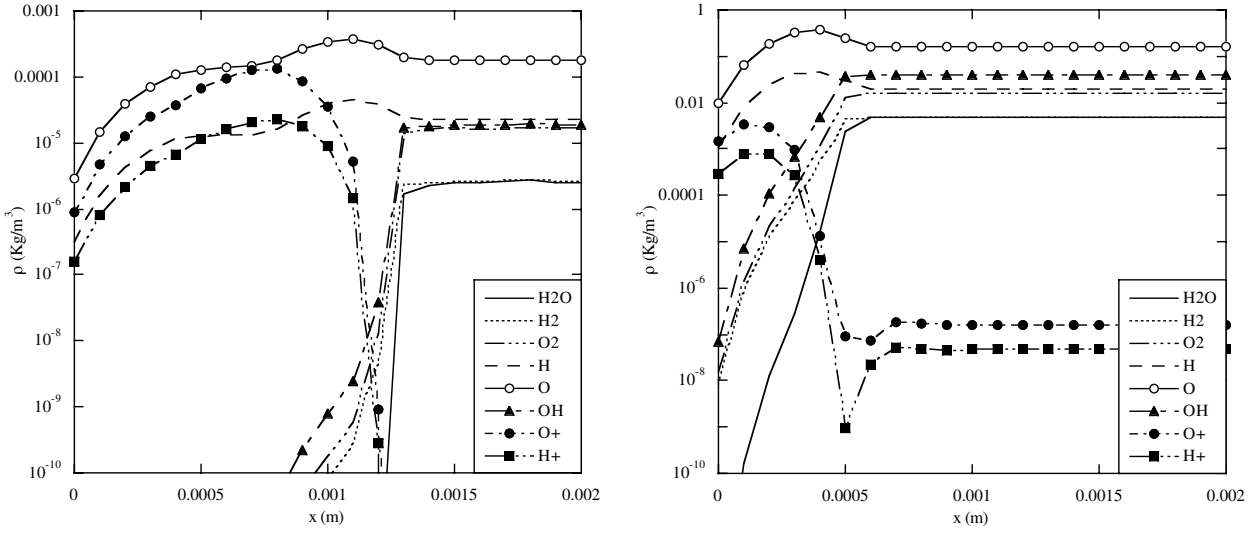

Fig. 9 Density profile of H_2O, H_2, O_2, H, O, OH, O^+, and H^+ as a function of distance from the target after 5×10^{-8} s from the beginning of the laser pulse along the normal in the middle of the target. The expansion occurs in water vapor background at 10^{-3} atm (Fig. 8a) and at 1 atm (Fig. 8b).

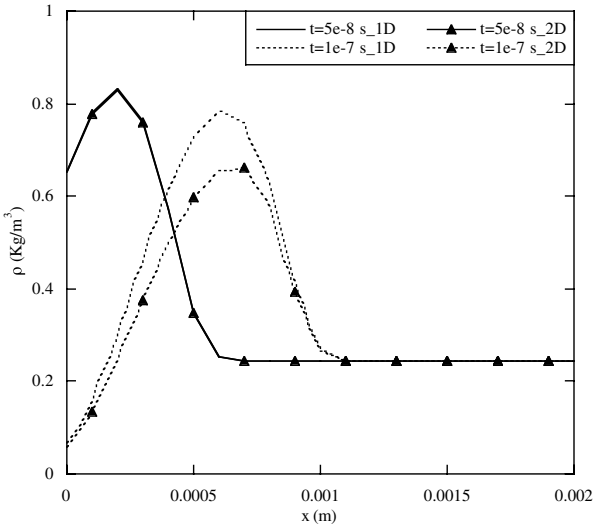

Fig. 10 Density profile as a function of distance from the target after 5×10^{-8} s and 10^{-7} s from the beginning of the laser pulse. Comparison between 1-D and 2-D results, obtained along the normal in the middle of the target. The expansion occurs in water vapor background at 1 atm.

(Fig. 9a), the presence of ions is more incisive than in the case of a higher background pressure (Fig. 9b). Finally, the broadening of the plume is shown in Fig. 10, comparing a 2-D calculation with a monodimensional Euler code. At the beginning, discrepancies between the two codes are quite small, but as time goes on the introduction of a bidimensional code is fundamental.

IV. Conclusions

The theoretical modeling of a plasma expansion occurring in different background at different pressure has been carried out. The fundamental role of a 2-D fluid-dynamic code in the case of simulations running for time much longer than the laser pulse duration has been shown. Moreover, the effect of chemical processes in local thermodynamic equilibrium is discussed, showing also the influence of different environments. The global heat capacity (frozen and reactive) strongly affects the dynamics of the plume expansion. Two-dimensional calculations make it possible to simulate the emission spectra accounting also for self-absorption. However, the local thermodynamic equilibrium assumption is valid only in high pressure environment. The equilibrium and free-flow calculations can be considered as extreme cases for finite rate chemical kinetics. A kinetic model for finite rate kinetics has been already investigated in 1-D fluid dynamics [3,29] and will be applied to 2-D models in the future.

Acknowledgments

This work has been supported by Miur Firb n. RBAU01H8FW "Dinamica Microscopica Della Reattività Chimica" and by CAST (Configurazioni Aerotermodinamiche Innovative per Sistemi di Trasporto Spaziale).

References

[1] Willmott, P. R., and Huber, J. R., "Pulsed Laser Vaporization and Deposition," *Reviews of Modern Physics*, Vol. 72, No. 1, 2000, pp. 315–328. doi:10.1103/RevModPhys.72.315

[2] Giardini, A., Marotta, V., Morone, A., Orlando, S., and Parisi, G. P., "Thin Films Deposition in RF Generated Plasma by Reactive Pulsed Laser Ablation," *Applied Surface Science*, Vols. 197–198, Sept. 2002, pp. 338–342. doi:10.1016/S0169-4332(02)00395-1

[3] Capitelli, M., Casavola, A., Colonna, G., and De Giacomo, A., "Laser-Induced Plasma Expansion: Theoretical and Experimental Aspects," *Spectrochimica Acta B*, Review, Vol. 59, No. 3, 2004, pp. 271–289. doi:10.1016/j.sab.2003.12.017

[4] Bogaerts, A., Chen, Z., and Gijbels, R., "Laser Ablation for Analytical Sampling: What Can We Learn from Modeling?," *Spectrochimica Acta Part B*, Vol. 58, No. 11, 2003, pp. 1867–1893. doi:10.1016/j.sab.2003.08.004

[5] Le, H. C., Zeitoun, D. E., Parisse, J. D., Snetis, M., and Marine, W., "Modeling of Gas Dynamics for a Laser-Generated and Propagation into Low-Pressure Gases," *Physical Review E*, Vol. 62, No. 3, 2000, pp. 4152–4161. doi:10.1103/PhysRevE.62.4152

[6] Colonna, G., Casavola, A., and Capitelli, M., "Modelling Plasma LIBS Expansion," *Spectrochimica Acta B*, Vol. 56, No. 6, 2001, pp. 567–586. doi:10.1016/S0584-8547(01)00230-0

[7] Casavola, A., Colonna, G., De Giacomo, A., De Pascale, O., and Capitelli, M., "Experimental and Theoretical Investigation of Laser-Induced Plasma of a Titanium Target," *Applied Optics*, Vol. 42, No. 30, 2003, pp. 5963–5969. doi:10.1364/AO.42.005963

[8] De Giacomo, A., Shakhatov, V. A., Senesi, G. S., and Orlando, S., "Spectroscopic Investigation of the Technique of Plasma Assisted Pulsed Laser Ablation of Titanium Dioxides," *Spectrochimica Acta B*, Vol. 56, No. 8, 2001, pp. 1459–1472. doi:10.1016/S0584-8547(01)00274-9

[9] Kelly, R., "Gas Dynamics of the Pulsed Emission of a Perfect Gas with Applications to Laser Sputtering and to Nozzle Expansion," *Physical Review A*, Vol. 46, No. 2, 1992, pp. 860–873. doi:10.1103/PhysRevA.46.860

[10] Amoruso, S., "Modeling of UV Pulsed-Laser Ablation of Metallic Targets," *Applied Physics A: Solids and Surfaces*, Vol 69, No. 3, 1999, pp. 323–332. doi:10.1007/s003390051008

[11] Chrisey, D. B., and Huber, G. K., *Pulsed Laser Deposition of Thin Films*, Wiley-Interscience, New York, 1994.

[12] Russo, R. E., Mai, X., Liu, H., Gonzalez, J., and Mao, S. S., "Laser Ablation in Analytical Chemistry—A Review," *Talanta*, Vol. 57, No. 3, 2002, pp. 425–451. doi:10.1016/S0039-9140(02)00053-X

[13] Capitelli, F., Colao, F., Provenzano, M. R., Fantoni, R., Brunetti, G., and Senesi, N., "Determination of Heavy Metals in Soils by Laser Induced Breakdown Spectroscopy," *Goederma*, Vol. 106, Nos. 1–2, 2002, pp. 45–62. doi:10.1016/S0016-7061(01)00115-X

[14] Noll, R., Bette, H., Brysch, A., Kraushaar, M., Monch, I., Peter, L., and Sturm, V., "Laser-Induced Breakdown Spectroscopy—Applications for Production Control and Quality Assurance in the Steel Industry," *Spectrochimica Acta B*, Vol. 56, No. 6, 2001, pp. 637–649. doi:10.1016/S0584-8547(01)00214-2

[15] Knight, A. K., Scherbarth, N. L., Cremers, D. A., and Ferris, M. J., "Characterization of Laser Induced Breakdown Spectroscopy (LIBS) for Application to Space Exploration," *Applied Spectroscopy*, Vol. 54, No. 3, 2000, pp. 331–340. doi:10.1366/0003702001949591

[16] Borgia, C., Burgio, L., Corsi, M., Fantoni, R., Palleschi, V., Salvetti, A., Squarcialupi, M. C., and Tognoni, E., "Self-Calibrated Quantitative Elemental Analysis by Laser-Induced Plasma Spectroscopy: Application to Pigment Analysis," *Journal of Cultural Heritage*, Vol. 1, No. 6, 2000, pp. S281–S286. doi:10.1016/S1296-2074(00)00174-6

[17] Lopez-Moreno, C., Palanco, S., Javier Laserna, J., De Lucia, F.C., Jr., Miziolek, A. W., Rose, J., Walters, R. A., and Whitehouse, A. I., "Test of a Stand-Off Laser-Induced Breakdown Spectroscopy Sensor for the Detection of Explosive Residues On Solid Surfaces," *Journal of Analytical Atomic Spectrometry*, Vol. 21, No. 1, 2006, pp. 55–60. doi: 10.1039/b508055j.

[18] De Giacomo, A., Dell'Aglio, M., Colao, F., and Fantoni, R., "Double Pulse Laser Produced Plasma on Metallic Target in Seawater: Basic Aspects and Analytical Approach," *Spectrochimica Acta B*, Vol. 59, No. 9, 2004, pp. 1431–1438. doi:10.1016/j.sab.2004.07.002.

[19] Kumar, A., Yueh, F. Y., and Singh, J. P., "Double-Pulse Laser-Induced Breakdown Spectroscopy with Liquid Jets of Different Thicknesses," *Applied Optics*, Vol. 42, No. 30, 2003, pp. 6047–6051. doi:10.1364/AO.42.006047

[20] Rai, V. N., Yueh, F. Y., and Singh, J. P., "Study of Laser-Induced Breakdown Emission from Liquid Under Double Pulse Excitation," *Applied Optics* Vol. 42, No. 12, 2003, pp. 6047–6051. doi:10.1364/AO.42.006047

[21] Fichet, P., Mauchien, P., Wagner, J. F., and Moulin, C., "Quantitative Elemental Determination in Water and Oil by Laser Induced Breakdown Spectroscopy," *Analytica Chimica Acta*, Vol. 429, No. 2,

2001, pp. 269–278.
doi:10.1016/S0003-2670(00)01277-0

[22] Nakamura, S., Ito, Y., and Sone, K., "Determination of an Iron Suspension in Water by Laser Induced Breakdown Spectroscopy with Two Sequential Laser Pulses," *Analytical Chemistry*, Vol. 68, No. 17, 1996, pp. 2981–2986.
doi:10.1021/ac9601167

[23] Pichahchy, A. E., Cremers, D. A., and Ferris, M. J., "Elemental Analysis of Metals Under Water Using Laser-Induced Breakdown Spectroscopy," *Spectrochimuca Acta Part B*, Vol. 52, No. 1, 1997, pp. 25–39.
doi:10.1016/S0584-8547(96)01575-3

[24] Pearman, W., Sacffidi, J., and Angel, S. M., "Dual-Pulse Laser Induced Breakdown Spectroscopy in Bulk Acqueous Solution with an Orthogonal Beam Geometry," *Applied Optics*, Vol. 42, No. 30, 2003, pp. 6085–6106.
doi:10.1364/AO.42.006085

[25] Kennedy, P. K., Hammer, D. X., and Rockwell, B. A., "Laser Induced Plasma in Aqueous Media," *Progress in Quantum Electronics*, Vol. 21, No. 3, 1997, pp. 155–248.
doi:10.1016/S0079-6727(97)00002-5

[26] De Giacomo, A., Dell'Aglio, M., and De Pascale, O., "Single-Pulse Laser Induced Plasma Spectroscopy in Aqueous Solution," *Applied Physics A: Solids and Surfaces*, Vol. 79, Nos. 4–6, 2004, pp. 1035–1038.
doi:10.1007/s00339-004-2622-1

[27] Casavola, A., De Giacomo, A., Dell'Aglio, M., Taccogna, F., Colonna, G., De Pascale, O., and Longo, S., "Experimental Investigation and Modelling of Double Pulse Laser Induced Plasma Spectroscopy Under Water," *Spectrochimica Acta B*, Vol. 60, Nos. 7–8, 2005, pp. 975–985.
doi:10.1016/j.sab.2005.05.034

[28] Brennen, C. E., *Cavitation and Bubble Dynamics*, Oxford Univ. Press, Oxford, England, U.K., 1995.

[29] Casavola, A., Colonna, G., De Giacomo, A., and Capitelli, M., "Laser Ablation of Titanium Metallic Targets: Comparison Between Theory and Experiment," *Journal of Thermophysics and Heat Transfer*, Vol. 17, No. 2, 2003, pp. 225–231.

[30] Casavola, A., Colonna, G., De Giacomo, A., and Capitelli, M., "A Combined Fluid Dynamic and Chemical Model to Investigate the Laser Induced Plasma Expansion," *Applied Physics A: Materials Science & Processing*, Vol. 79, Nos. 4–6, 2004, pp. 1315–1317.

[31] Kennedy, P. K., Hammer, D. X., and Rockwell, B. A., "Laser Induced Plasma in Aqueous Media," *Progress in Quantum Electronics*, Vol. 21, No. 3, 1997, pp. 155–248.
doi:10.1016/S0079-6727(97)00002-5

[32] De Giacomo, A., Dell'Aglio, M., Colao, F., Fantoni, R., and Lazic, V., "Double-Pulse LIBS in Bulk Water and on Submerged Bronze Samples," *Applied Surface Science*, Vol. 247, Nos. 1–4, 2005, pp. 157–162.
doi:10.1016/j.apsusc.2005.01.034

[33] Chrisey, D. B., and Huber, G. K., "Pulsed Laser Deposition of Thin Films," *Wiley-Interscience*, New York, 1994.

[34] D'Angola, A., Colonna, G., Gorse, C., and Capitelli, M., "Thermodynamic and Transport Properties in Equilibrium Air Plasmas in a Wide Pressure and Temperature Range," *European Physical Journal D* (to be published).

[35] Hilsenratt, J., and Klein, M., "Tables of Thermodynamic Properties of Air in Chemical Equilibrium Including Second Virial Corrections from 1500 K to 15000 K," AEDCTR-65-58, 1965.

[36] Capitelli, M., and Ficocelli Varracchio, E., "Thermodynamic Properties of Ar-H2 Plasmas," *Revue Internationale Des Hautes Temperatures Et Des Refractaires,*, Vol. 14, No. 4, 1977, pp. 195–200, Rapide Not 12:29.

[37] Sevast'yanov, M., and Chernyavskaya, R. A., "Virial Coefficients of Nitrogen, Oxygen, and Air at Temperatures from 75 to 2500°k," *Journal of Engineering Physics and Thermophysics*, Vol. 51, No. 1, 1986, pp. 851–854.
doi:10.1007/BF00871372

[38] Lesieur, M., Comte, P., and Zinn-Justin, J., Les Houches, Session LVIX, "Mecanique des Fluides Numerique Computational Fluid Dynamics," edited by M. Lesieur, P. Comte, and J. Zinn-Justin, 1993, pp. 5–63.

[39] Birman, A., Har'El, N. Y., Falcovitz, J., Ben-Artzi, M., and Feldman, U., "Operator-Split Computation of 3-D Symmetric Flow," *22nd International Symposium on Shock Waves*, Imperial College, London, U.K., 18–23 July 1999; also Paper 3461.

[40] Landau, D. L., and Lifshitz, E. M., *Statistical Physics*, Pergamon, Oxford, England, U.K., 1986.

[41] Herzberg, K. G., *Molecular Spectra and Molecular Structure-I. Spectra of Diatomic Molecules*, Van Nostrand, Princeton, 1950.

[42] Capitelli, M., Colonna, G., Giordano, D., Marraffa, L., Casavola, A., Minelli, P., Pietanza, L., and Taccogna, F., "Tables of Internal Partition Functions and Thermodynamic Properties of High-Temperature Mars-Atmosphere Species from 50 K to 50000 K," edited by D. Giordano, and B. Warmbein, Vol. ESA STR-246, 1-267, Isbn: 92-9092-349-0, European Space Agency Publications, Estec. Noordwijk, The Netherlands, 2005.

[43] Colonna, G., and D'Angola, A., "A Hierarchical Approach for Fast and Accurate Equilibrium Calculation," *Computer Physics Communications*, Vol. 163, No. 3, 2004, pp. 177–190.
doi:10.1016/j.cpc.2004.08.004

[44] Colonna, G., "Improvements of Hierarchical Algorithm for Equilibrium Calculation," *Computer Physics Communications* (to be published).